ELSEVIER

Journal of Structural Geology 25 (2003) 2141–2157

JOURNAL OF STRUCTURAL GEOLOGY

www.elsevier.com/locate/jsg

Very high strains recorded in mylonites along the Alpine Fault, New Zealand: implications for the deep structure of plate boundary faults

Richard J. Norris*, Alan F. Cooper

Department of Geology, University of Otago, PO Box 56, Dunedin, New Zealand

Received 26 September 2002; accepted 14 February 2003

Abstract

Oblique displacement on the Alpine Fault, which forms the principal structure along the Australian–Pacific plate boundary in South Island, New Zealand, has resulted in exhumation of a kilometre-wide mylonite zone in the hanging wall adjacent to the current brittle fault trace. The mylonites formed under amphibolite facies conditions at depths of ca. 25 km and have been uplifted during the past 5 Ma. A suite of 65–70 Ma pegmatite veins in the hanging wall Alpine schists has been progressively deformed within the mylonite zone and sheared out over a strike length of ca. 100 km. Measurements of the thickness distribution of the pegmatite veins within the non-mylonitised schists and at three localities within the progressively strained mylonites have been used to estimate strain values within the mylonites. The thicknesses approximate a log-normal distribution, with a mean value that is progressively reduced through the protomylonites, mylonites and ultramylonites. By assuming that the thickness distribution currently observed in the schists was the same for the pegmatites within the mylonites before strain, a model of deformation incorporating simple shear and simultaneous pure shear is used to strain the undeformed veins until a fit is obtained with the strained distributions. Shear strains calculated range from 12 to 22 for the protomylonites, 120 to 200 for the mylonites and 180 to 300 for the ultramylonites, corresponding to pure shear values of 1–3 in each case. These values are compatible with the strains predicted if most of the surface displacement on the fault over the past 5 Ma were accommodated within a 1–2-km-wide mylonite zone through the middle and lower crusts. The results suggest that processes such as erosional focussing of deformation and thermal weakening may cause intense strain localisation within the lower crust, with plate boundary deformation restricted to narrow zones rather than becoming increasingly distributed over a widening shear zone with depth.

Keywords: Mylonites; Strain; Fault structure; Alpine Fault

1. Introduction

The nature of the deep structure of major faults is an important problem (Lynch and Richards, 2001), and the degree to which slip observed on the fault at the surface is localised into zones of intense ductile strain at depth is difficult to determine. Do they continue down through the middle crust as a zone of highly localised intense shear or does the strain rapidly dissipate outwards into a broad zone of distributed deformation in the lower crust (e.g. Prescott and Nur, 1981; Zandt, 1981; Sibson, 1983; Weijermars, 1987).

Certainly most structural geologists would interpret major mylonite zones that occur within exhumed deep crustal rocks (e.g. Great Slave Lake shear zone, Canada: Hanmer, 1988; South Armorican shear zone: Berthé et al., 1979; Woodroffe Thrust mylonite zone, Australia: Bell, 1978; Camacho et al., 1995) to represent the deep parts of major crustal faults. Many of these zones are tens of kilometres in width (e.g. Berthé et al., 1979; Weijermars, 1987; Hanmer, 1988). However, without any real knowledge of what the upper crustal fault zone looked like, it is possible that the motion occurred over a relatively broad zone of anastomosing faults. The common occurrence of anastomosing shear zones over wide areas of metamorphic rocks (e.g. Jiang and White, 1995; Davison et al., 1995) might suggest a model of broadening of strains at depth into a semi-continuous deforming lower crust. Even narrow upper crustal fault zones, like the Alpine Fault, may broaden rapidly at depth so that, although still underlain by a mylonite zone in which some localised plastic shear has occurred, a substantial part of the total slip has been distributed into a wide zone of ductile strain within more typical lower crustal tectonites. Unfortunately, because the fault structures overlying these mylonite zones are largely

* Corresponding author. Tel.: +64-3-479-7520; fax: +64-3-479-7527.
E-mail address: richard.norris@stonebow.otago.ac.nz (R.J. Norris).

0191-8141/03/$ - see front matter © 2003 Elsevier Ltd. All rights reserved.
doi:10.1016/S0191-8141(03)00045-2

absent today, we cannot reconstruct an individual fault zone throughout the crust (cf. Sibson, 1977; Sibson et al., 1979). Sibson (1983) and Hanmer (1988) present possible models for the deep structure of fault zones that outline some of these possibilities.

Measurement of strain in mylonite is difficult and there are few published examples. Shear strains >100 for example would result in all objects of known original shape being rendered unrecognisable, and all pre-existing features rotated into parallelism. Most published strain determinations in mylonites (e.g. Mawer, 1983; Bailey et al., 1994) have been based on measurements of the shape of deformed grains such as quartz or the shapes of feldspar porphyroclasts. A problem here is that, after relatively small strains, the original grains will have been recycled several times and the original grain outlines will no longer be recognisable. Not surprisingly, therefore, the shear strains recorded in these studies are fairly low, of the order of 1–5, although most appear to be flattening rather than simple shear strains, suggesting a strong component of transpression (e.g. Fossen and Tikoff, 1998). Wenk (1998) measured deformed xenoliths in a mylonitised granite within the Santa Rosa mylonite zone of California. He calculated extensions of up to 10 which, if produced by simple shear, would correspond to a shear strain also of

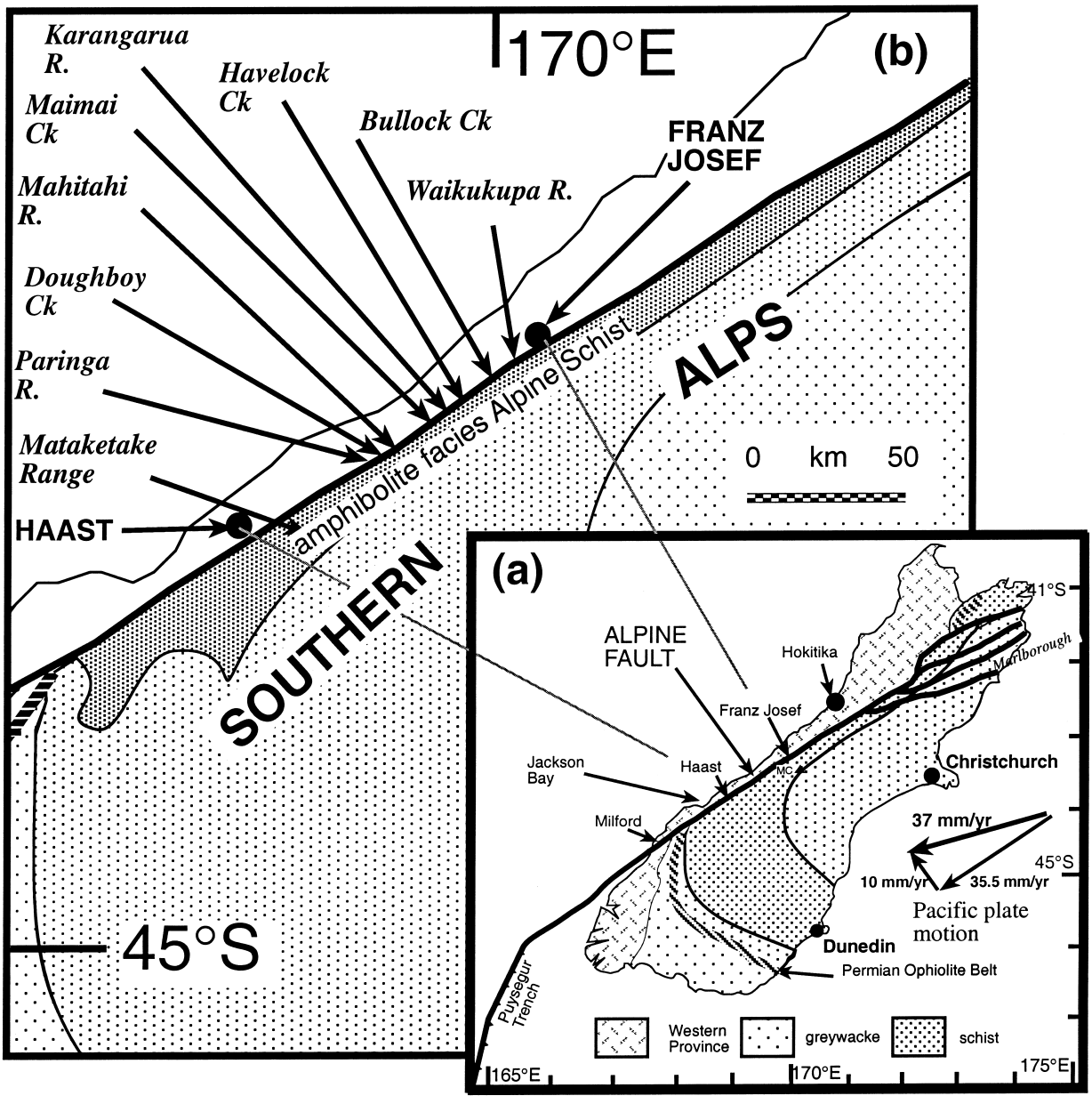

Fig. 1. (a) Map of South Island, New Zealand, showing main features of the Australian–Pacific plate boundary, including Alpine Fault, Puysegur trench, and Marlborough fault system. The Pacific plate motion relative to the Australian plate is from the modified Nuvel-1 solution of Demets et al. (1994), and is calculated for the central South Island. Components parallel and perpendicular to the Alpine Fault are also shown. (b) More detailed map of central South Island showing localities referred to in text. The black line representing the Alpine Fault roughly corresponds in thickness to the mylonite zone.

ca. 10. Once again, the strains plot in the flattening field rather than a plane strain expected for simple shear. Choukroune and Gapais (1983) also used deformed xenoliths to estimate strains in mylonites within the Aar granite of the central European Alps and obtained values equivalent to a shear strain of up to five, although again, the strains tended to plot in the flattening field. Boullier (1986) measured shear strains of up to 20 in the late Pan-African Abeibara-Rarhous shear zone in Mali from the deflection of foliation and the change in thickness of layering. The high shear strains were measured over a zone 500 m wide, which resulted in a calculated displacement of 4 km, an order of magnitude less than recorded on the related brittle faults. Weijermars (1987) described the Palomares shear zone of southern Spain as widening downwards from a narrow brittle fault to a ductile shear zone some 45 km wide at a depth of 20 km. Shear strains estimated were between one and two. Lacassin et al. (1993) used boudinaged veins to measure extension in mylonites within the Oligo-Miocene Red River-Ailao Shear Zone in southeast Asia. Assuming simple shear, shear strains of up to 33 were recorded over an 8–10 km zone, giving a total displacement of more than 300 km. In this latter case, the mylonites do seem to be related to major crustal faults and to accommodate the bulk of the surface displacement.

In few of these examples were the mylonites able to be linked with a single high strain-rate plate boundary fault like the Alpine Fault. In this paper, we use the changes in thickness of a suite of pegmatite veins that are progressively deformed within the mylonites on the Alpine Fault to estimate total shear strains values. Our results show that the strains within the mylonite zone are compatible with the high shear strains expected if the mylonites indeed accommodate the bulk of the displacement at depth.

2. Alpine Fault

The Alpine Fault cuts through the western side of the South Island, New Zealand, and is the main manifestation of the Australian–Pacific plate boundary (Fig. 1; Norris et al., 1990). Estimates of Late Quaternary slip rates (Norris and Cooper, 2001) and contemporary strain accumulation measured by GPS surveys (Beavan et al., 1999) indicate that the Alpine Fault accommodates around two-thirds to three-quarters of the 37 ± 2 mm/yr of plate motion calculated from the Nuvel 1A global plate model (DeMets et al., 1994). The orientation of the interplate slip vector is approximately 20° to the trace of the fault so that the total plate motion may be recalculated into components of 35.5 mm/yr parallel and 10 mm/yr perpendicular to the fault. Norris and Cooper (2001) have shown that motion on the fault within its central portion is approximately parallel to the interplate vector with components of both strike-slip and dip-slip. The dip-slip component as a proportion of the perpendicular component of interplate motion reduces to the northeast and southwest, and falls to zero on the far southwestern part of the fault south of Jackson Bay (Fig. 1; Norris and Cooper, 2001). Estimates of rates of strike-slip on the fault are consistent with a constant rate along its length of 27 ± 6 mm/yr (Norris and Cooper, 2001). Reconstruction of plate motions through the late Cenozoic indicates a total convergence across the South Island of some 70–90 km (Walcott, 1998).

Recent geophysical traverses across the central South Island (SIGHT programme; Davey et al., 1998) have shown that the depth to the Moho approximately doubles from ca. 20 km off the east coast to 40 km under the Southern Alps. Part therefore of the total convergence has been accommodated by crustal thickening forming a deep root (also see Woodward, 1979). Walcott (1978) argued that the geodetically measured strain across the South Island is accommodated by ductile distributed creep across a broad zone. The slip data on the Alpine Fault indicate that this can only be true near surface for, at most, ca. 25% of the predicted plate motion. Molnar et al. (1999) and Stern et al. (2000) have suggested, based on mantle anisotropy, that at depth, New Zealand overlies a broad zone of shear some 200 km wide and localisation onto faults only occurs in the brittle crust. Bourne et al. (1998) have produced a similar model to interpret the geodetic data from Marlborough, northeast of the Alpine Fault.

Deep seismic reflection profiles in other parts of the world have imaged faults cutting the deep crust, even the Moho (e.g. McGeary, 1989; Flack et al., 1990; McBride et al., 1996), whereas other profiles suggest some faults do not extend as resolvable features into the lower crust (e.g. Lynn et al., 1983; Hauge et al., 1987). A short CDP reflection line east of the Alpine Fault was reported by Davey et al. (1995) who recognised reflections dipping at 50° in line with the surface trace of the Alpine Fault and extending to a depth of over 25 km. They interpreted these as representing the extension of the Alpine Fault zone into the lower crust.

Because of the component of convergence across the Alpine Fault, the hanging wall has been uplifted and rocks from over 20 km depth have been exhumed within the last few million years (Cooper, 1980; Adams, 1981; Holm et al., 1989). A zone up to 1 km wide of mylonite and protomylonite is exposed adjacent to the fault east of the surface trace (Reed, 1964; Sibson et al., 1979). The degree of mylonitisation increases inhomogeneously westwards across the zone from amphibolite facies schist protolith in the east, to protomylonite, mylonite, and ultramylonite adjacent to the active fault trace. The mylonitic rocks have been deformed under amphibolite facies conditions at depths of 20–30 km (Holm et al., 1989; Grapes and Watanabe, 1992, 1994). The Alpine Fault is unusual, therefore, in having its deep-seated mylonite zone exhumed alongside the currently active surface trace and its associated cataclastic rocks (Sibson et al., 1979). We have here, therefore, a rare opportunity to study the deep-seated part of a currently active fault whose surface dimensions

and structure we already know and whose slip rate and slip direction we can determine.

In the case of the Alpine Fault, we can definitely say that a narrow zone of faulting with a slip rate of around 27 mm/yr at the surface overlies a mylonite zone 1–2 km wide originally developed at a depth of 20–30 km. A question remains, however, as to how much of the surface slip rate is accommodated within the mylonites. It is quite feasible that, although they undoubtedly represent a zone of localised strain, the mylonites may none-the-less only accommodate a small proportion of the total displacement.

The mylonites have been uplifted from depth during the last 5 Ma since the plate boundary became significantly convergent (Sutherland, 1995). During that time, assuming a constant average slip rate of 27 mm/yr (Sutherland, 1994; Norris and Cooper, 2001), a total of some 135 km of displacement should have accrued on the fault. Displacement in the top 10 km or so of the crust is likely to be by cataclasis and frictional sliding and not contribute to the ductile strain exhibited by the mylonites. For a steady rate of uplift, therefore, mylonite exhumed from 30 km depth will have accumulated ductile strain for about two-thirds of its uplift history. If all the slip recorded on the fault at the surface has been accommodated at depth within a 1-km-wide mylonite zone, the presently exposed mylonites should have taken up about 90 km by ductile shearing, which gives an average shear strain of ca. 90. The higher strained parts of the mylonite zone should exhibit considerably more than this.

3. Pegmatites

3.1. Occurrence

Thick (0.5– > 30 m) pegmatite veins have been known from the Mataketake Range north of Haast (Fig. 1) for many years and were exploited commercially for mica during World War 2 (Wellman, 1947). Books of muscovite and biotite greater than 10 cm in diameter and 5 cm thick occur in the thicker pegmatites (Fig. 2). The pegmatites occur within amphibolite facies Alpine Schist and their mineralogy (quartz, plagioclase, K-feldspar, muscovite, biotite, garnet) suggests they formed from wet partial melts under similar metamorphic conditions to the host rocks (Wallace, 1974; Chamberlain et al., 1995). The pegmatites have been dated by U/Pb measurements on zircon and monazite at 65–70 Ma (Chamberlain et al., 1995; Batt et al., 1999). Ar/Ar and fission track data from Batt et al. (1999) suggest they remained deep in the crust until being exhumed during late Cenozoic convergence in the last 5 Ma. Contrary to previous accounts (e.g. Wellman, 1947; Wallace, 1974), the pegmatites on the Mataketake Range are not generally concordant with foliation. Some are closely parallel, some are at a low angle, and some are perpendicular to the enclosing schist foliation (Figs. 2 and 3). The pegmatites have been weakly deformed, particularly along their margins with the schist, and appear to be folded on a macroscopic scale by folds corresponding to the Haast Antiform and Thomas Synform (Cooper, 1974). These folds are considered on other grounds to be late Tertiary in age (Cooper et al., 1987). The veins do not exhibit any extensive penetrative deformation, however, nor do they have any indications of mylonitic deformation.

Fig. 2. (a) Semi-concordant pegmatite vein on Mataketake Range. Late quartz veins within the pegmatite are prominent. Width of photo ca. 2 m. (b) Discordant pegmatite vein on Mataketake Range. Strike of schist foliation runs approximately left to right across the photo.

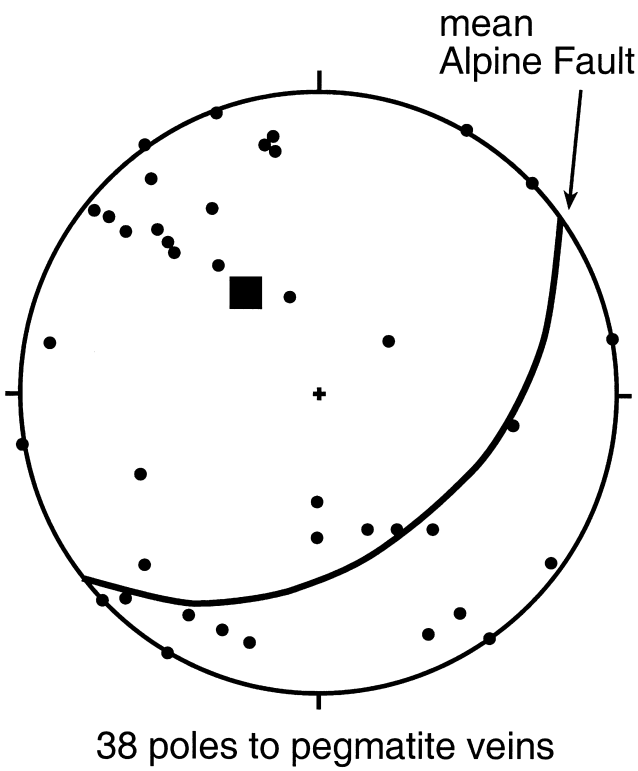

Fig. 3. Equal area sterogram of poles to pegmatite veins on the Mataketake Range. Although scattered, there are roughly equal concentrations sub-perpendicular and sub-parallel to the mean Alpine Fault plane.

North of the Mataketake Range, similar pegmatites are found in the eastern margins of the Alpine Fault mylonite zone at Paringa River and Doughboy Creek (Fig. 1b). Here they are quite recognisable, with some veins still over a metre thick. They exhibit a penetrative mylonitic fabric, however, with the feldspars reduced to augen (Fig. 4b).

We have found pegmatites within the mylonite zone in all the major creeks we have explored between Paringa River and Franz Josef, a strike length of around 100 km (Fig. 1). At Paringa River and Doughboy Creek, the pegmatites occur within the protomylonites, but farther north, at Mahitahi River, Havelock, Maimai and Bullock Creeks, they lie within the mylonites proper. At Waikukupa River, the northernmost occurrence of the pegmatite swarm, the veins, now completely concordant with the mylonitic foliation, occur within ultramylonite adjacent to the cataclasite zone along the fault (Norris and Cooper, 1997). Thus the pegmatites appear to form a continuous band within the mylonite zone for nearly 100 km along strike and cross progressively from the eastern margin protomylonites to the western margin ultramylonites over this distance. Associated with the pegmatites are a thick series of amphibolites (metabasites) and these too can be traced continuously over the same distance. Together with the pegmatites, these provide evidence that a specific sequence of rock units within the hanging wall has been progressively sheared along strike through the mylonites for 100 km as a semi-continuous band. These observations also demonstrate that the precursor rocks to the mylonites at any point are to be found, not in the immediate hanging wall, but up to 100 km or so further southwest.

The degree of deformation of the pegmatites increases markedly as they extend into the more highly strained mylonites and the thickness of the veins diminishes until individual pegmatite veins are commonly only 1–10 cm thick (Fig. 5). They are still recognisable as pegmatites, however, as they retain feldspar augen and large flakes of muscovite commonly in excess of 5 cm in diameter, even within a pegmatite layer less than 2 cm thick. (The microstructure of the pegmatites is currently under investigation. Preliminary observations indicate that large biotite flakes survive into the protomylonites but recrystallise at higher strains, whereas large books of muscovite deform mainly by slip along [001] to form large mica fish, and appear resistant to recrystallisation.)

The progressive deformation of the pegmatites suggests a way of estimating strain in the mylonites. Although the pegmatites in the Mataketake Range are variable in thickness, they range between 0.5 and 30 m with some type of continuous frequency distribution. At Waikukupa River, the pegmatite layers range from <1 to 10 cm in

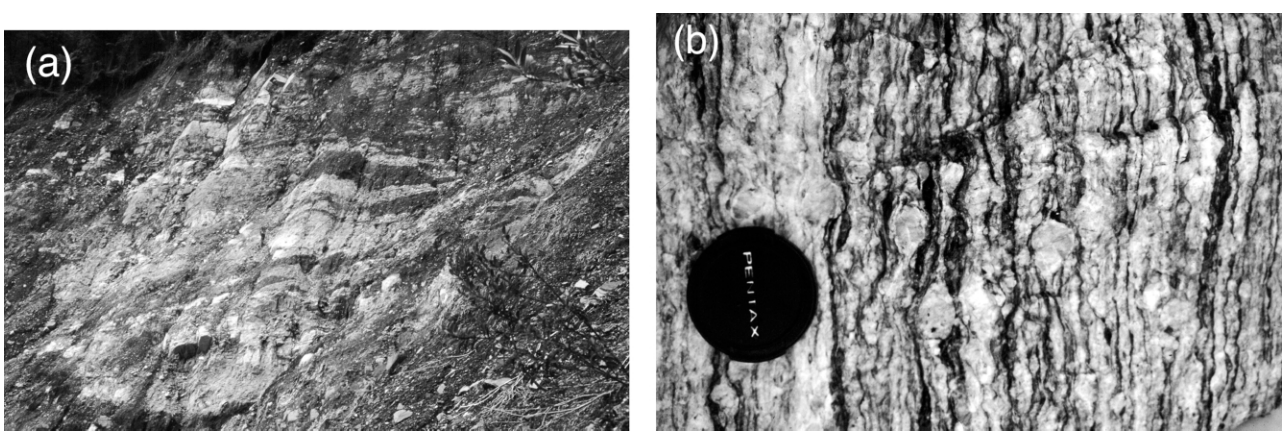

Fig. 4. (a) Deformed pegmatite veins in protomylonites, Doughboy Creek. Face is approximately 10 m high. Note large-scale isoclinal folding of some veins. (b) Mylonitised pegmatite showing augen structure, Doughboy Creek.

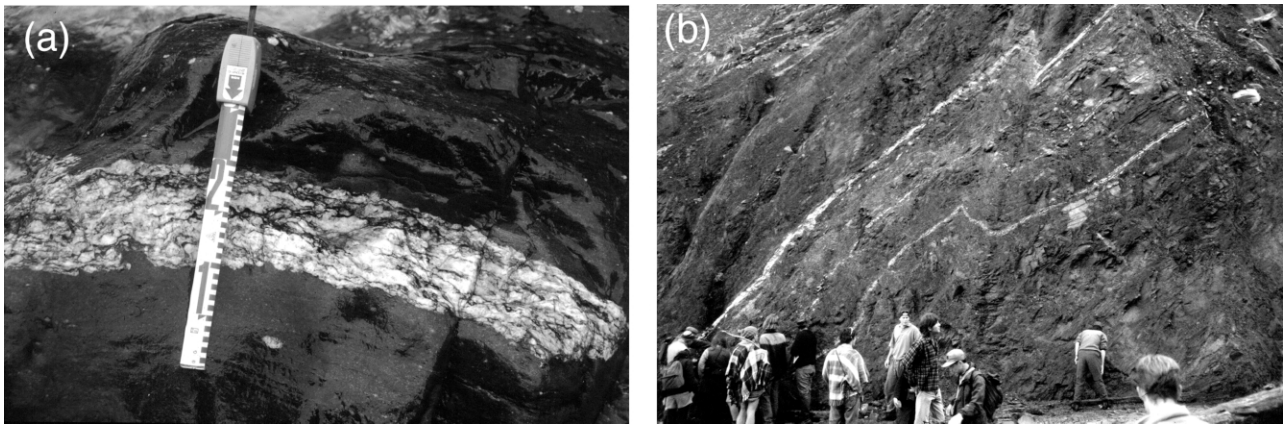

Fig. 5. (a) Highly strained pegmatite vein approximately 10 cm thick, within mylonites, Mahitahi River area. (b) Highly attenuated pegmatites within ultramylonite ca. 50 m above basal Alpine Fault plane, Waikukupa River. Pegmatites show good continuity despite extreme attenuation.

thickness, again with some type of frequency distribution. If the changes in thickness distribution of the pegmatites can be quantified, then it should be possible to derive an estimate of the strain within the mylonite zone.

3.2. Measurement techniques

3.2.1. Mataketake Range

The Mataketake Range pegmatites occur outside of the mylonite zone and so form the starting point for estimating mylonite strain. The Range has a relatively flat top at about 1000 m elevation with abundant rock outcrops through the tussock grassland. Measurements were made of the thickness of all pegmatite veins encountered during a series of traverses across the range top. It is possible that there is a slight bias towards thicker veins as these tend to be more obvious and form resistant outcrops, whereas thinner veins may possibly be covered in vegetation. Nevertheless, as thorough a sampling as possible was made and a total of 55 veins were measured.

3.2.2. Doughboy Creek/Paringa River

Doughboy Creek, north of the Paringa River (Fig. 1), exposes a good section through the deformed pegmatites within the protomylonite zone (Fig. 4). The bulk of the outcrop, however, several hundred metres east of the present trace of the Alpine Fault, occurs high up on a 100-m-high face and is difficult to access. We measured veins in three ways. We were able to gain access to parts of the face and measured all veins observed. We measured the thicknesses of a series of veins in part of the face using a stadia telescope and a range-finder. Finally, we measured thicknesses of veins enclosed in large fallen blocks at the foot of the face. Although not ideal, we consider that the sampling was fairly random without any major bias being introduced. A total of 73 veins was measured, including six from the Paringa River, which were included in the dataset as they occur in a similar part of the mylonite zone and are very close to Doughboy Creek. One of the features of the pegmatites at Doughboy Creek is that some of the thick veins exhibit large isoclinal folds (Fig. 4a). It is not unlikely that, during the early stages of deformation, some veins would become folded, given that many veins in the Mataketake Range would be at a high angle to the mylonite zone (Fig. 3). Whether the folding is due to buckling and flattening of a more competent layer or whether it is due to variations in shearing across the vein is not determined.

3.2.3. Mahitahi/Maimai/Havelock Creeks

Measurements from these three creeks were made in outcrop, most of which were at least 100 m from the present fault trace. At Mahitahi River (Fig. 5a), the pegmatites were found high up in a tributary creek (Makatata Stream) north of the main valley, as the main river lacks exposure of mylonite, as does the major valley of the Karangarua River. Due to incomplete outcrop, insufficient measurements were obtained from any one of these three localities to form independent datasets. Vein thickness ranges from each creek were similar, however, and all occurred within good mylonite, and so we have combined them into a single dataset of 82 measurements.

3.2.4. Waikukupa River

A large slip on the true left (i.e. south) bank of the Waikukupa River downstream of the bridge exposes the basal part of a large overthrust sheet of mylonite and cataclasite (Norris and Cooper, 1997). Deformed pegmatites occur within the basal ultramylonites (Fig. 5b) less than 100 m above the basal fault surface. Continuous exposure allowed collection of a single set of 52 thickness measurements. Because the strain is very great, the thinner pegmatites tend to exhibit pinch and swell features. The thicker part of the vein was measured in such cases, not the thinned neck. Isolated feldspar augen and large flakes of mica within the mylonite suggest that complete disruption and mylonitisation of some veins has occurred so that they are no longer recognisable. The data therefore may be biased towards the thicker veins.

4. Results

The measurements are plotted as thickness against frequency as histograms on log-normal plots (Fig. 6). The interval width is 0.5. The data have also been smoothed by use of a running mean with a similar window width as the histograms (0.5) but calculated every 0.1 interval (Fig. 6).

All four datasets show roughly similar bell-shaped distributions with a progressive reduction in mode with increasing distance northwards from the Mataketake Range. The data can be fitted by a log-normal distribution curve shown as an overlay on the plots in Fig. 6. The fit of a log-normal distribution is good for the Waikukupa and Mahitahi datasets but less acceptable for the Doughboy and Mataketake data. Many veins and dykes in nature appear to conform to a log-normal distribution (e.g. McCaffrey et al., 1993), whereas others have described power-law (fractal) distributions, particularly from metamorphic segregation veins (Manning, 1994; Clark et al., 1995). A power-law distribution is no better fit to the Mataketake Range data than is a log-normal distribution (Fig. 6), and is a worse fit to the datasets from the other localities. Although not essential for the purposes of strain estimation (since we use the actual distribution rather than a model one), the log-normal distribution is a fair description of the datasets and can be characterised by the mean and standard deviation (Fig. 6).

The log-means of the four datasets decrease from 3.27 (1860 mm) for Mataketake, 2.31 (200 mm) for Doughboy, 1.35 (22 mm) for Mahitahi, to 1.17 (15 mm) for Waikukupa. The standard deviations are roughly similar (0.595, 0.616) for Mataketake and Doughboy and somewhat smaller (0.38, 0.444) for the more highly strained sites at Mahitahi and Waikukupa. The Mahitahi/Maimai/Havelock combined dataset has a noticeably smaller spread (Fig. 6)—this could conceivably be due to re-sampling the same subset of veins at all three localities since the outcrop was limited at each. On the other hand, the distribution does not have a skewed character, which might be expected if there were any major bias in the sampling.

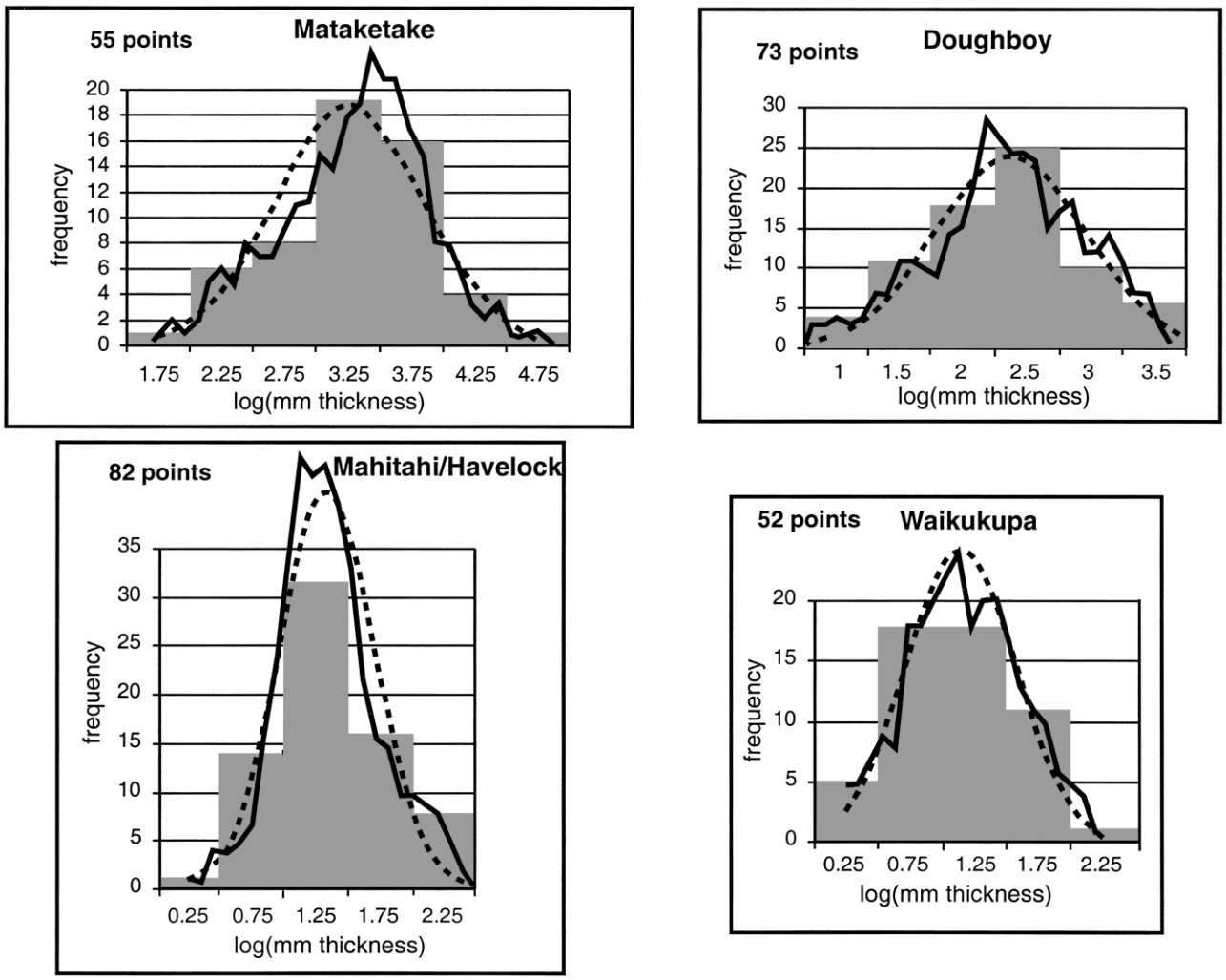

Fig. 6. Frequency-thickness data from pegmatites plotted on log-normal graphs. Heavy continuous line is smoothed distribution based on a moving average with a 0.5 window calculated at 0.1 intervals. Dashed line is best-fit normal distribution.

5. Strain calculations

The decrease in the mean thickness of pegmatites from the four localities is systematic with qualitative estimates of the increase in strain in the mylonites. The Mataketake Range pegmatites show no mylonitic deformation, the Doughboy samples are within the eastern part of the mylonite zone where the mylonites are dominantly lower strain proto-mylonites, the Mahitahi/Maimai/Havelock suite are within high strain, strongly foliated mylonites and the Waikukupa examples are from fine-grained ultramylonites. The systematic reduction in mean thickness with increasing strain suggests that the thickness distribution may be used to calculate the amount of strain in the mylonites.

5.1. Assumptions

To use the thickness distributions to calculate strain, a number of assumptions have to be made. Some are made because there is no alternative, whereas others are made to simplify the procedure and because more complex assumptions are unjustified at present. The assumptions are: (1) measurements of thickness of veins at each locality provide a reasonably representative and unbiased sample of the actual thickness distribution; (2) the pegmatites in the Mataketake Range have not suffered any mylonitic deformation and represent the original thickness distribution of the pegmatite veins at each of the other localities prior to mylonitisation; (3) strain at each locality is approximately homogeneous and the pegmatites have strained homogeneously within the country rock mylonite; (4) we can specify the type of strain (simple shear, transpression, etc.) that has produced the mylonite zone; and (5) we can make some assumption about the original orientations of the veins.

Each of these assumptions is questionable and needs justification. None is completely justifiable and hence the resulting strain estimates remain model strains only. We will attempt to argue that they are based on reasonable, if not proven, assumptions.

We discuss in the previous section the procedures for measurement and the character of the data. We have measured as many veins as we could find at each locality. We can only assume that they are reasonably representative while allowing that some bias may occur. Perhaps the most important source of bias is due to complete destruction of the thinner veins in the more highly deformed datasets. This would shift the distribution to a higher mean and reduce the spread. In this case, the strain would be underestimated, and perhaps all strains should be viewed as minima due to this problem.

The pegmatites in the Mataketake Range, as described above, show no mesoscopic or microscopic evidence for mylonitic deformation and neither do the surrounding schists. Whether the vein sets at the other localities had the same thickness distribution prior to mylonitisation is impossible to tell. One observation that may be relevant is that, even in very thin veins at Waikukupa (measured as only a few millimetres thick), plates of muscovite several centimetres in diameter are found, and books of muscovite over one centimetre thick occur in most of the veins. In the Mataketake Range, only the thicker pegmatites (>2 m) contain such large books of mica and in all veins, the mica books are very much smaller than the vein thickness. The fact that very large flakes of muscovite are found in very thin, highly deformed pegmatite veins strongly suggests that these were originally thick veins like those presently exposed on the Mataketake Range. Feldspar augen in the mylonitised pegmatites are also very large in proportion to the vein thickness and in the most deformed veins, single augen are as wide as the thickest part of the vein. This is in marked contrast to the Mataketake Range where grain-size is roughly proportional to vein thickness. These observations suggest that the mylonitised sequences represent the deformed equivalents of a set of pegmatites similar to those on the Mataketake Range.

The third assumption is that of homogeneous strain, both at a locality scale and within each pegmatite. The first part of this assumption is necessary since we are using a whole set of veins for the calculation. Equally clearly, however, deformation in the mylonites is not homogeneous and intercalated higher and lower strain zones exist, with lenses of lower strain material wrapped around by ultramylonites on a metre scale. Nevertheless, there is a clear progression through the mylonite zone from low strain mylonites in the east to high strain ultramylonites in the west (Sibson et al., 1979; Prior, 1988). Some degree of inhomogeneity must exist but we contend that the pegmatite veins nevertheless reflect the average amount of strain in their particular part of the mylonite zone. The second part of the assumption, that the pegmatites have deformed homogeneously with the matrix, is necessary for the calculation. It is probably not precisely true as suggested by isoclinal folding in some pegmatites at Doughboy Creek (Fig. 4a). Nevertheless, strongly developed boudinage and pinch and swell structures are not evident in the pegmatite veins until they are reduced to the thickness of one feldspar augen.

Assumptions 4 and 5 are required to develop a strain model. Because the pegmatites only provide a measure of shortening perpendicular to the veins, they cannot be used to differentiate different types of strain such as simple shear, pure shear, pure flattening, or some combination (e.g. Fossen and Tikoff, 1998). The procedure we adopt is to take a set of veins with a thickness distribution like that in the Mataketake Range and with some initial distribution of orientations, and deform it by some specified strain, recalculate the thickness distribution, and compare it with those of the mylonitised pegmatites. By varying the types of strain combinations and orientations, their respective effects can be tested. (We have not attempted to use the change in orientations of the veins in our strain calculations because,

at the high strains encountered in the mylonites, all veins are effectively parallel to the mylonitic foliation.)

5.2. Strain model

Orientations of veins in the Mataketake Range are generally steep, mainly sub-parallel or sub-perpendicular to the foliation with some scattered orientations in between. Initially, therefore, we assume a set of vertical veins evenly spread in orientation with a thickness distribution like that in the Mataketake Range (Fig. 6; Appendix A). We consider a combination of simple shear parallel to the mylonite zone and a shortening normal to the mylonite zone (Fossen and Tikoff, 1998). The Alpine Fault dips at 40–60° south-eastwards and, in the study area, the slip is oblique in orientation so that it accommodates both boundary-parallel and boundary-normal plate motion. We have run our model with the pure shear extension direction normal to the shear direction, parallel to the shear direction, and as a pure flattening with equal extension in both directions. These variations made very little difference to the strain values calculated, which were mainly sensitive to the amount of shortening normal to the zone. For simplicity, therefore, we adopt a model of shear parallel to the fault zone, shortening normal to it with extension perpendicular to the shear direction (i.e. Fossen and Tikoff, 1998, type B; cf. Sanderson and Marchini, 1984).

We calculate the deformation for different combinations of simple and pure shear using the simultaneous shearing formulation of Fossen and Tikoff (1993). Details of the procedure are given in Appendix A. We apply a given strain to a set of veins with the Mataketake thickness distribution and calculate the new thickness distribution that results. The resulting distributions also have bell-shaped forms (Fig. 7). We compare these with the measured distributions from the deformed vein sets and choose the strain combinations that produce the best fit with the measured thickness distributions (Fig. 7). We emphasize, however, that the data do not allow us to determine the relative proportions of pure shear and simple shear. There are a wide range of combinations that would equally fit the data. If we increase the pure shear component, we decrease the simple shear and vice versa. We need to narrow down the range from other arguments.

Many high-grade mylonite zones have been interpreted as products of combined flattening and simple shear (e.g. Hanmer et al., 1992, 1995; Wenk, 1998). The nature of the strain in these rocks may be reflected in the type of fabrics developed. Thus a simple shear-dominated deformation might be expected to produce L–S tectonites (Flinn, 1965). Lineations are developed throughout the Alpine Fault mylonites to various degrees. They tend to be stronger in the lower strain protomylonites and are commonly quite weakly developed in the higher strain, fine-grained mylonites and ultramylonites. In the latter, however, certain lithologies are strongly lineated, and coarser units, such as the pegmatites themselves, develop strong lineations. It is not clear that fabrics in these highly deformed rocks reflect the total strain in a simple manner, as a great deal of recycling of grains has taken place (cf. Piazolo and Passchier, 2002). Microstructures indicate strong non-coaxial deformation with a constant sense of shear. Further work on the microstructures is currently in progress.

In the case of the Alpine Fault mylonites, the value of the pure shear component we contend is likely to be low. The mylonite zone is rarely more than a kilometre in width and extends for several hundred kilometres along a major fault that has a total of more than 450 km of dextral strike-slip. Shear sense indicators within the mylonites are extremely consistent, showing dextral-reverse shear (e.g. Sibson et al., 1979; Prior, 1988; Little et al., 2002; authors' unpublished observations). Assuming constant volume, any shortening normal to the zone resulting in thinning must be accommodated by extension of the zone horizontally or vertically (Dewey et al., 1998; Jiang et al., 2001). Major horizontal extension of the mylonites seems unlikely given the length of the fault, the parallelism of the mylonites and their relatively constant thickness over a strike length of several hundred kilometres (e.g. this contrasts with the Striding-Athabasca shear zone described by Hanmer et al. (1995)). It is most likely, therefore, that any thinning of the zone is accommodated by vertical extension, as suggested by Jiang et al. (2001). The hanging wall schists have been extended vertically and show strong transpressive fabrics (Holcombe and Little, 2001) (Note that the vorticity estimates ($W_k = 0.12–0.3$) of Holcombe and Little (2001) apply only to the low-strain hanging wall schists and not to the mylonites.) The amount of late Cenozoic flattening in these schists measured by Holcombe and Little (25–50%) is commensurate with a doubling of the thickness of the crust beneath the Southern Alps (Davey et al., 1998). If the extension within the narrow mylonite zone were substantially greater than that in the hanging wall schists, the mylonites would be extruded at the surface and there would need to be a reversal in shear sense across the zone (cf. Dewey et al., 1998). Such features are not observed (Prior, 1988; Little et al., 2002).

We suggest that any vertical extension due to pure shear must be of a similar magnitude (i.e. ca. 2) to that exhibited by the hanging wall schists (a similar argument was used by Lacassin et al. (1993) in their studies of the Red River-Ailao mylonite zones). We have therefore calculated models for combinations of simple shear with pure shear components of 1, 2 and 3, to investigate their effect (Table 1). In general, the greater the pure shear component, the less the corresponding simple shear component (note that the simple shear component, γ, for simultaneous pure shear and simple shear, is intermediate in value between that required to obtain the same finite strain from a simple shear followed by a pure shear and that for a pure shear followed by a simple shear (Fossen and Tikoff, 1993)). End member strains of

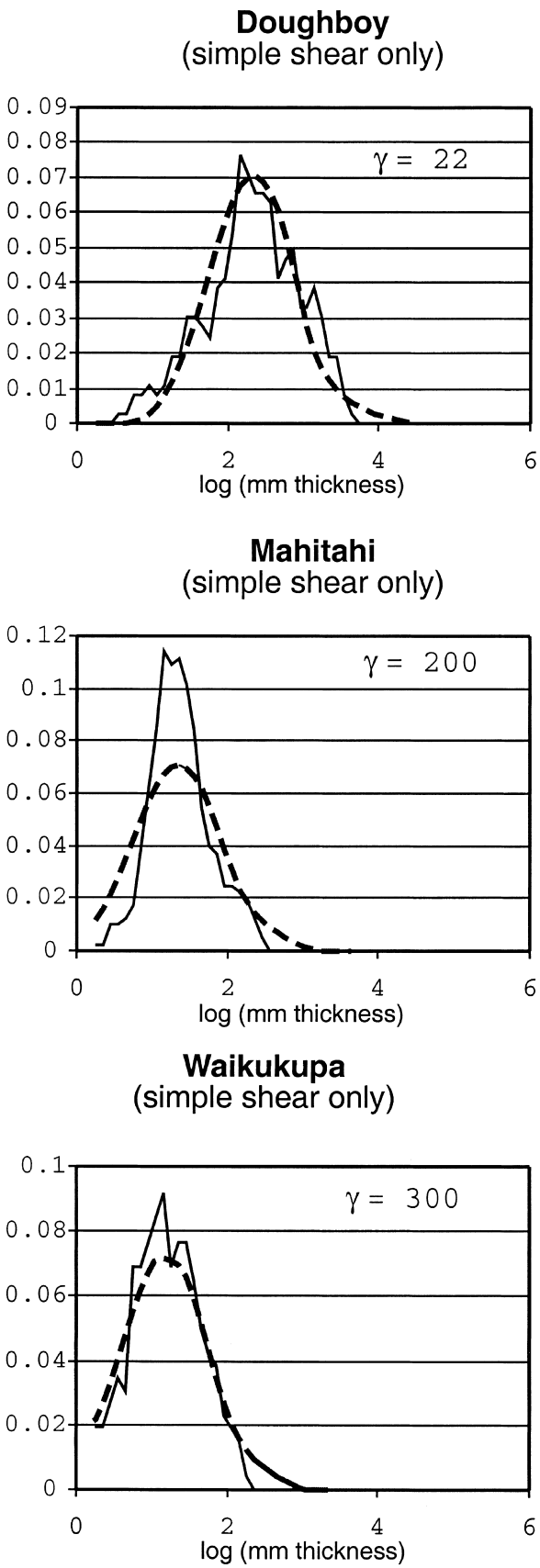

Fig. 7. Best-fit calculated strained distributions (heavy dashed line) and smoothed frequency-lognormal thickness distributions of pegmatites from Fig. 6 for each of the main measured groups. The frequency has been normalised for comparison. The calculated distribution shown is for simple shear only. Adding a pure shear component reduces the amount of simple shear but the shape and fit of the calculated curve is the same.

Table 1
Values of simple shear strain (γ) parallel to the x axis corresponding to different values of pure shear strain (α = extension parallel to the z axis) for best-fit solutions to the datasets from localities within the mylonite zone

Locality	$\alpha = 1$	$\alpha = 2$	$\alpha = 3$
Doughboy	22	15	12
Mahitahi/Havelock	200	150	120
Waikukupa	300	220	180

entirely pure shear or entirely simple shear have similar values.

The results show that for the range of values of pure shear assumed (1–3), the simple shear strain values recorded by the pegmatite thickness distributions range from 12 to 22 for the protomylonites of the Doughboy area, to 180–300 for the ultramylonites of the Waikukupa. These strains are extremely high, an order of magnitude higher than most of those recorded from mylonites in the literature (e.g. Mawer, 1983; Lacassin et al., 1993; Wenk, 1998).This statement is true whatever values of pure shear are assumed.

To test the sensitivity to the initial orientations chosen, the model was run with concentrations in one or more orientations instead of a uniform spread. As long as there were two concentrations more or less at right angles with a scattering in between (similar to the actual orientations on the Mataketake Range; Fig. 3), the differences between these and a uniform distribution were $<10\%$. Only if there was a single strong concentration did the results deviate markedly from those assuming a uniform pattern.

We conclude therefore that the changes in thickness distributions recorded in the pegmatites in the mylonite zone are the result of extremely large shear strains probably in excess of 150 and maybe as high as 300 in the ultramylonites. We acknowledge that we have had to make a number of assumptions, but do not consider these unreasonable. The robust observation is that the average thickness of the veins changes over several orders of magnitude, and provided the deformed pegmatites had a roughly similar thickness distribution as the Mataketake Range sample, the strain has to be extremely high, whatever its exact nature.

6. Discussion

6.1. The Alpine Fault Zone at depth

Small earthquakes east of the Alpine Fault extend to

around 10 km depth (Leitner et al., 2001) suggesting that displacement in the top 10 km or so of the crust is probably brittle sliding during earthquakes. Presumably the cataclasites and gouge zones along the Alpine Fault result from this style of deformation. Within this zone, the mylonites are cataclastically deformed and otherwise passively translated. The ductile shear strains that we are recording must have developed below this level, as also indicated by the amphibolite facies assemblages within the mylonites. Since the highest strained ultramylonites occur right against the current active trace, it is likely that a part of the mylonite zone is attached to the footwall at depth and has not yet been exhumed. The total width over which strain is accumulating could therefore be as much as double the mylonite width at the surface if the original mylonite zone was symmetrical about the ultramylonites, although this is not necessary and asymmetrical exhumation may be more likely (e.g. Davis et al., 1986). The eastern margin of the mylonites is gradational into schist and therefore is likely to represent the original boundary of the zone. It could be argued that the mylonite zone is much wider at depth and the presently exposed width is due to truncation during uplift. Variations in its exposed width may indeed be due to this reason, but a much greater variation in the exposed width of the zone, with large lenses several kilometres across, might be expected if the observed mylonite zone were but tectonic slices of a much wider zone at depth.

The exact distribution of strain across the mylonite zone is not provided by the three strain estimates here. As an illustration (Fig. 8), we model the fault as 0–100 m ultramylonites (Waikukupa), 100–300 m mylonite (Mahitahi) and 300–1000 m protomylonite (Doughboy). The exact thickness of the protomylonites is less critical than

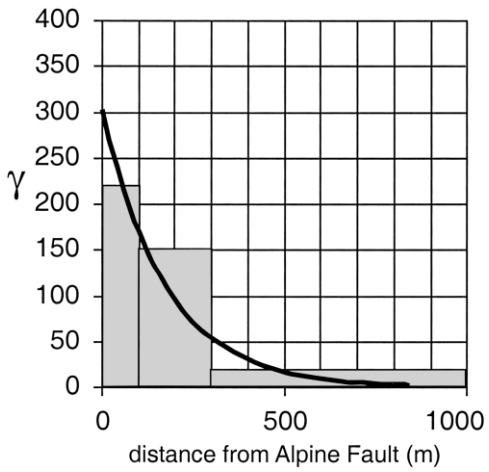

Fig. 8. Models of strain distribution across the mylonite zone. The shaded histogram assumes average shear strain values as calculated for a pure shear strain (α) of two (Table 1), for a shear zone with an ultramylonite thickness of 100 m, a mylonite thickness of 200 m and a protomylonite thickness of 700 m. The heavy black curve is an exponential distribution fitted through points at 0 m (shear strain = 300) and at 500 m (shear strain = 1). Integrating the two models gives total offset for the exhumed part of the mylonite zone of 62.5 and 55 km, respectively (see text for discussion).

that of the ultramylonites, but the latter is difficult to estimate with any certainty due to variation along such a long section of fault, so the model remains approximate only. Assuming this distribution, the total offset across the exposed mylonite zone works out at about 85 km for a simple shear only model and about 60 km for a transpressional model with a pure shear component of 2. If we allow for the possibility that up to half the mylonite zone is still attached to the footwall and not exposed, the figures could be as high as 170 and 120 km, respectively. An alternative model is to assume an exponential curve to represent the strain distribution across the mylonite zone (cf. Boullier, 1986), with a shear strain maximum of 300 at the fault and 1 at 1 km from the fault. Integrating this curve gives a total offset of 55 km, or a maximum of 100 km across a doubled thickness. These estimates must be viewed circumspectly as they could easily be modified by changing the strain distribution across the whole mylonite zone. Nevertheless, they provide some idea of how much slip on the Alpine Fault could be accommodated within the deep-seated mylonite zone.

The time at which the mylonites started forming is open to question. However, the main convergence across the Alpine Fault has really only been going on for the last 5 Ma or so (Sutherland, 1994). If these rocks were at a depth of say 30 km initially, and there has been 70–90 km of total convergence since then (Walcott, 1998), it follows that the mylonites we see today at the surface must have formed during the last 5 Ma. This is supported by very young fission track ages on zircon (Tippett and Kamp, 1993) and Ar/Ar dates on micas and amphiboles (Adams, 1981; Chamberlain et al., 1995; Batt et al., 1999). If the mylonites have simply been translated through the top 10 km by brittle sliding, then they will have been undergoing ductile shear for about two-thirds of the time since 5 Ma. At an average rate of slip on the fault of 27 mm/yr (Sutherland, 1994; Norris and Cooper, 2001), up to 90 km of ductile shear, therefore, may have accumulated within the presently exposed mylonite zone. The calculated displacement across the mylonite zone from the strain estimates, even given the large uncertainties, is clearly compatible with the amount of slip on the Alpine Fault. Therefore, this narrow zone of ductile shear, 1–2 km wide, is able to accommodate all the slip on the Alpine Fault at depth. This represents extreme localisation of strain and means that the fault should be represented by a very narrow localised shear zone to depths of the order of 25–30 km. It is presumably this intensely deformed zone that is imaged by the seismic reflections reported by Davey et al. (1995).

Seismic profiles do not provide any indication that the Alpine Fault penetrates the Moho as a single fault zone. The growth of the root suggests that, below some depth, considerable distributed deformation has occurred in the lowermost crust. The lack of rocks of higher grade than amphibolite facies at the surface even after 70–90 km of convergence also suggests that the highly localised movement within the mylonite zone is dissipated at some level in

the crust. There is some suggestion that the fault zone may flatten at depth (Wellman, 1979; Norris et al., 1990; Davey et al., 1995) and act as a detachment surface for the top 25–30 km above the root. This concept has been used in the dislocation models of Beavan et al. (1999). Nevertheless, the data reported here suggest that a large part of the interplate motion rapidly becomes localised into a narrow ductile shear zone in the middle crust. The results reported here, therefore, do not directly refute the views of Molnar et al. (1999) and Stern et al. (2000) of a broad 200-km-wide zone of continuous shear within the underlying mantle, but they do suggest a significant change in style of displacement between the mantle lithosphere and the crust.

The mechanisms by which such strong localisation takes place are somewhat speculative. Koons (1990) and Beaumont et al. (1992) have shown how strongly asymmetric erosion patterns across an orogen may focus deformation into a narrow zone. Rapid exhumation of hot rocks along such a relatively narrow zone will lead to localised thermal weakening (Koons, 1987). Such feedback mechanisms may eventually result in a highly localised ductile shear zone at depth (Ellis et al., 2001; Koons et al., 2003). Another question, partly related, concerns the common assumption that flow in the mantle and lower crust drives brittle faulting in the upper crust, which is merely a passive reflector of deeper flow (e.g. Bourne et al., 1998). Recently, however, Maggi et al. (2000) have questioned the assumption of high strength upper mantle and have suggested that most of the lithospheric strength lies in the upper crust. In this scenario, it may be the localisation of deformation along major faults in the upper crust, which localises deformation below them rather than the other way round (cf. Ellis et al., 2001; Jackson, 2002). Localisation of strain in the upper crust will lead to higher stresses in the middle crust below (White, 1996; Ellis and Stöckhert, 2002) and this in turn will lead to higher local strains. If the rocks undergo strain softening, a positive feedback loop will lead eventually to a highly focussed fault zone through the crust. Sutherland et al. (2000) have argued that the line of the Alpine Fault was initially controlled by the old rifted margin of the Resolution Ridge. This old line of weakness coupled with the feedback mechanisms discussed above, may have led to the intense localisation of ductile strain at depth.

6.2. Significance for plate boundary fault zones

A number of different models for the deep structure of fault zones have been proposed in the literature. Scholz (1988) illustrated a fault zone extending as a narrow shear zone to at least 25 km, as does Sibson (1977) based on observations of fault rocks. Imber et al. (2001) also propose a narrow zone of localised strain through the crust on the basis of observations of the exhumed Outer Hebrides Fault Zone. Prescott and Nur (1981) argue from geophysical data that the San Andreas Fault in the Coast Ranges is better modelled as a brittle fault above a wide zone of mid-crustal shear, although the seismic data used may not be adequate to image deep fault zones. Jones et al. (1994) suggest that the San Andreas Fault is terminated at the base of the seismogenic zone by a low-dipping zone of ductile shear. Schulz and Evans (2000) show that the Punchbowl Fault, an old trace of the San Andreas Fault, has a total width of around 200 m within the upper crust. This is supported by magnetotelluric measurements on the current San Andreas Fault by Unsworth et al. (1997) that image a narrow fault zone down to at least 8 km. The lower crustal structure of the fault, however, is less clear. Burchfiel et al. (1989) propose that the Altyn Tagh fault in Tibet terminates within a zone of mid-crustal shear and is confined to the upper brittle crust, whereas Wittlinger et al. (1998) present evidence for extension of the Altyn Tagh fault into the upper mantle. Lynch and Richards (2001) discuss some of the implications of different lower crustal models of fault zones, ranging from wide zones of distributed shear to narrow zones of concentrated shear strain, on the patterns of surface strain distribution and principal stress orientation during a single earthquake cycle.

Hanmer (1988) has attempted to reconstruct the deep structure of a fault zone from analysis of Great Slave Lake Shear Zone in the Canadian Shield. By observing the width of the zone exhibiting mylonitisation under granulite, amphibolite and greenschist faces, he argues for a shear zone that narrows and becomes more localised upwards, from 25 km wide in the lower crust to 1 km wide in the greenschist facies middle crust. Weijermars (1987) similarly suggested that the Palomares fault zone widens downwards into a ductile shear zone 45 km wide with shear strains of only 1–2 in magnitude. Boullier (1986) recorded shear strains of up to 20 across a 500-m-wide mylonite zone adjacent to a major late Precambrian fault in Mali. On the basis of a roughly exponential strain profile, she argued for a total width of 1 km at the level of exposure, but this still only gave an integrated displacement of 4 km compared with an order or two in magnitude greater displacement on the associated faults. Thus it is unlikely these mylonites represent the locus of fault movement at depth. Lacassin et al. (1993) describe a mylonite zone around 8–10 km wide adjacent to the Red River Fault and one of 5 km wide along the Wang Chao fault. Strain measurements within these shear zones are compatible with large fault displacements, but as the zones are much wider than the mylonites on the Alpine Fault, the strain values are less (up to 33). Nevertheless, the observations suggest localisation of fault movement at depth within a fairly narrow ductile shear zone.

A question is whether the Alpine Fault is a typical plate boundary fault or whether the degree of strain localisation at depth varies in different settings depending on a number of local factors such as those discussed above (e.g. localisation of erosion, degree and rate of exhumation of isotherms, total convergence, nature of rock material and upper crustal

structure, etc.). What the measurements presented here demonstrate is that, in some circumstances, strain at depth may be extremely localised within high strain mylonites beneath major fault zones, certainly through the mid-crust, and that mylonite zones may have an order of magnitude more shear strain than has generally been recorded.

One consequence of the measurements presented here is that the strain rate in the mylonites must have been extremely high. For a shear strain of say 300 over 5 Ma, a strain rate of ca. 10^{-12}/s is required. Calculated from another direction, 25 mm/yr over a zone 1 km in width also works out as a strain rate of around 10^{-12}/s. This rate is two orders of magnitude faster than rates commonly ascribed to geological deformation (e.g. Pfiffner and Ramsay, 1982; Weijermars, 1987) although strain rates of these magnitudes have been proposed previously for mylonite zones (e.g. Sibson, 1982; White, 1996). These high strain rates raise the question of deformation mechanisms responsible and whether a steady state creep can be assumed. If plastic instabilities arise at these strain rates (e.g. Hobbs et al., 1986; White, 1996), this could have important implications for the nucleation of earthquakes on such faults.

Acknowledgements

We thank Rick Sibson, Peter Koons, Tim Little, Dave Prior and Mark Walrond for discussions on many aspects of the Alpine Fault and its mylonites. We are grateful for constructive comments by the journal reviewers Simon

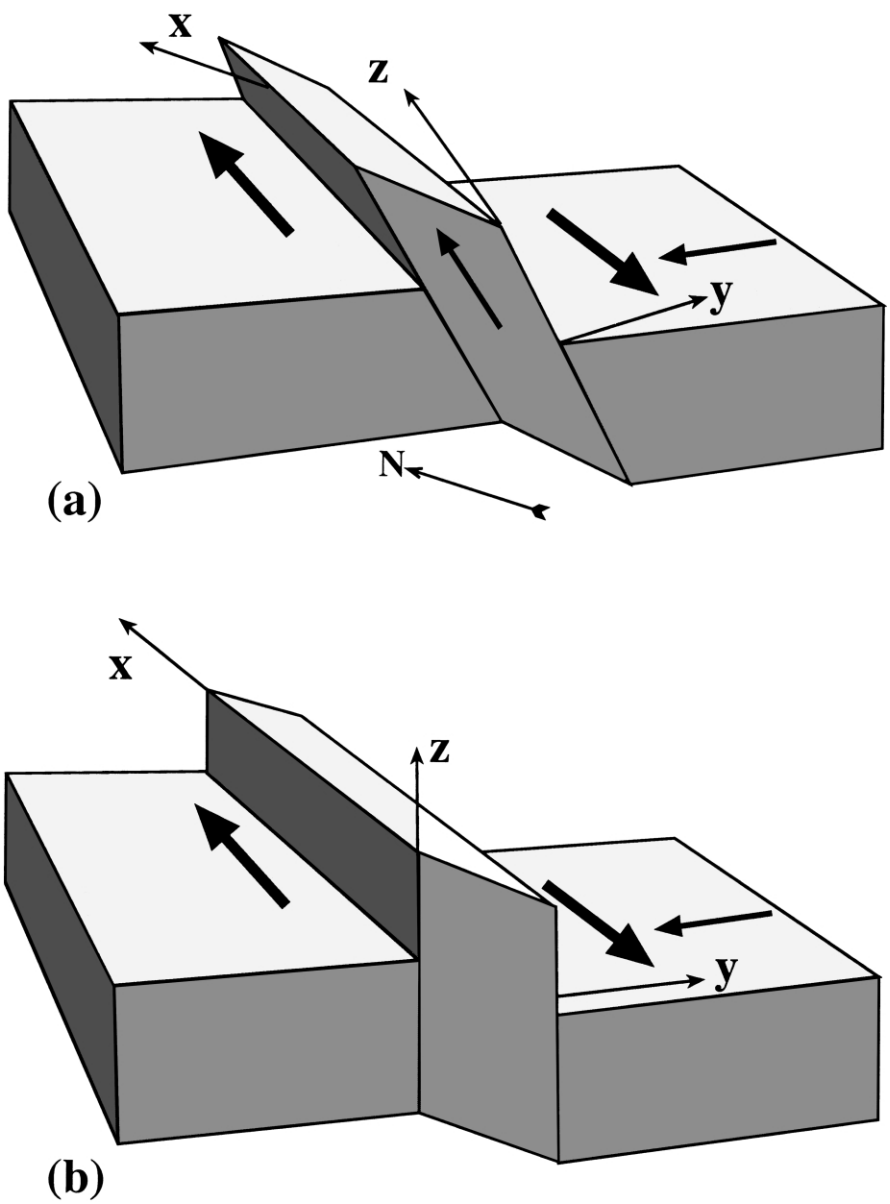

Fig. A1. (a) Shear zone model with co-ordinate axes in geographic orientation for the Alpine Fault. (b) Model rotated for convenience with axes vertical and horizontal. Model shown has pure shear extension parallel to z axis (Fossen and Tikoff, 1998, type B).

Hanmer and Michelle Markley and by editor Jim Evans. We of course remain responsible for the views expressed. The work was supported by the Public Good Science Fund of New Zealand.

Appendix A

The model developed here to calculate the changes in the thickness distribution of a set of veins is the simplest that can be justified by the data available. A shear zone is subjected to simple shear parallel to the zone and a simultaneous flattening perpendicular to it. For convenience, we here show (Fig. A1) the zone as vertical with the x axis parallel to the zone and horizontal, the y axis normal to the zone and the z axis vertical (in true geographic space, the Alpine Fault zone dips approximately 50°E, with the x axis plunging ca. 30°NE). A set of vertical veins with some predetermined orientation pattern (a uniform orientation was adopted but others were tested) is subjected to the imposed strain.

Consider a single vertical plane at angle θ to the x-axis (Fig. A2). The strain may be specified by the deformation matrix:

$$\begin{bmatrix} k_1 & \dfrac{\gamma(k_1-k_2)}{\ln(k_1/k_2)} & 0 \\ 0 & k_2 & 0 \\ 0 & 0 & k_3 \end{bmatrix} \tag{A1}$$

after Fossen and Tikoff (1993, Eqs. 17 and 19a), where γ is the simple shear strain parallel to the xz plane in the direction of the x-axis and k_1, k_2 and k_3 are the extensions/contractions parallel to the x, y and z axes, respectively.

Elongation of line OA is given by:

$$\sqrt{\lambda_A} = \sqrt{\left(\frac{k_1\cos\theta + \sin\theta\gamma(k_1-k_2)}{\ln(k_1/k_2)}\right)^2 + (k_2\sin\theta)^2}, \tag{A2}$$

and of OB by

$$\sqrt{\lambda_B} = k_3. \tag{A3}$$

As these two lines remain at right angles during strain,

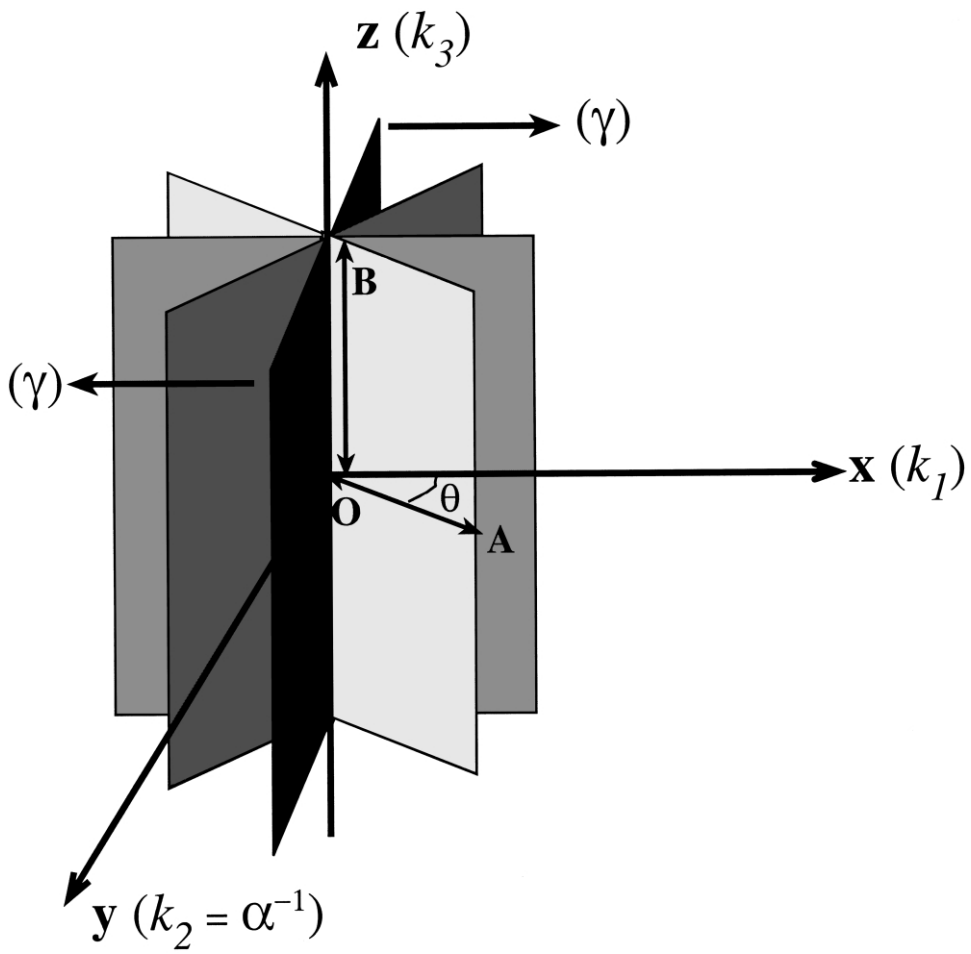

Fig. A2. Diagram showing model used for calculating thickness distribution after straining an initial thickness distribution. Initial distribution (e.g. Mataketake Range) is assumed to be uniform in orientation around z axis. xz plane represents shear plane, with simple shear component γ parallel to the x axis. A simultaneous pure shear component is applied with extensions k_1 parallel to x, k_2 parallel to y, and k_3 parallel to z. $k_2 = \alpha^{-1}$ parallel to the y-axis. Plane AOB makes an angle θ with the x axis.

the resulting strain perpendicular to the plane defined by them is:

$$\sqrt{\lambda_P} = (\lambda_A \lambda_B)^{-1/2} = \left[k_3 \sqrt{\left(\frac{k_1 \cos\theta + \sin\theta\gamma(k_1 - k_2)}{\ln(k_1/k_2)} \right)^2 + (k_2 \sin\theta)^2} \right]^{-1}. \quad \text{(A4)}$$

The log(final thickness) of a vein (l_1) of initial orientation θ and thickness l_0 is given by:

$$\log(l_1) = \log(l_0) - \log\left(\sqrt{\lambda_P}\right). \quad \text{(A5)}$$

Veins in each thickness category (interval of $\log(l_0) = 0.1$) were deformed for all values of θ (in intervals of 10°). The resulting thicknesses were weighted according to the proportion of veins in their original thickness category given by the thickness distribution of veins on the Mataketake Range, and the strained distribution of thicknesses calculated. This was then compared with the strained distributions measured in the field and the parameters adjusted until a good match was obtained. Constant volume was assumed (i.e. $k_1 k_2 k_3 = 1$) with shortening parallel to the y axis (k_2) equal to α^{-1}. The model was run with pure shear extension parallel to x axis ($k_1 = \alpha$, $k_2 = \alpha^{-1}$, $k_3 = 1$), parallel to the z axis ($k_1 = 1$, $k_2 = \alpha^{-1}$, $k_3 = \alpha$) and as flattening parallel to the y axis with equal extension on both x and z ($k_1 = \sqrt{\alpha}$, $k_2 = \alpha^{-1}$, $k_3 = \sqrt{\alpha}$). The different conditions did not make a great difference to the results as the values of α and γ mainly control the deformed thicknesses. The results reported in Table 1 are for a pure shear component with extension α parallel to the z axis (Fossen and Tikoff, 1998, type B). Note that the model is unable to differentiate between high α, low γ and low α, high γ. The reasons for taking values of $\alpha = 1$, 2 and 3 are given in the text.

References

Adams, C.J., 1981. Uplift rates and thermal structure in the Alpine Fault Zone and Alpine Schists, Southern Alps, New Zealand. In: McClay, K., Price, N.J.(Eds.), Thrust and Nappe Tectonics. Geological Society of London Special Publication 9, pp. 211–222.

Bailey, C.M., Simpson, C., De Paor, D.G., 1994. Volume loss and tectonic flattening strain in granitic mylonites from the Blue Ridge province, central Appalachians. Journal of Structural Geology 16, 1403–1416.

Batt, G.E., Kohn, B.P., Braun, J., McDougall, I., Ireland, T.R., 1999. New insight into the dynamic development of the Southern Alps, New Zealand, from detailed thermochronological investigation of the Mataketake Range pegmatites. In: Ring, U., Brandon, M., Lister, G., Willett, S. (Eds.), Exhumation Processes: Normal Faulting, Ductile Flow and Erosion. Geological Society of London Special Publication 154, pp. 261–282.

Beaumont, C., Fullsack, P., Hamilton, J., 1992. Erosional control of active compressional orogens. In: McClay, K.R., (Ed.), Thrust Tectonics, Chapman & Hall, London, pp. 1–18.

Beavan, J., Moore, M., Pearson, C., Henderson, M., Parsons, B., Bourne, S., England, P., Walcott, D., Blick, G., Darby, D., Hodgkinson, K., 1999. Crustal deformation during 1994–1998 due to oblique continental collision in the central Southern Alps, New Zealand, and implications for seismic potential of the Alpine fault. Journal of Geophysical Research 104, 25,232–25,255.

Bell, T.H., 1978. Progressive deformation and reorientation of fold axes in a ductile mylonite zone: the Woodroffe Thrust. Tectonophysics 44, 285–320.

Berthé, D., Choukroune, P., Jegouzo, P., 1979. Orthogneiss, mylonite, and non-coaxial deformation of granites: the example of the South Armorican shear zone. Journal of Structural Geology 1, 31–42.

Boullier, A.M., 1986. Sense of shear and displacement estimates in the Abeibara–Rarhous late Pan-African shear zone, Adrar des Iforas, Mali. Journal of Structural Geology 8, 47–58.

Bourne, S.J., Arnadottir, T., Beavan, J., Darby, D.J., England, P.C., Parsons, B., Walcott, R.I., Wood, P.R., 1998. Crustal deformation of the Marlborough fault zone in the South Island of New Zealand: geodetic constraints over the interval 1982–1994. Journal of Geophysical Research 103, 30147–30165.

Burchfiel, B.C., Quidong, D., Molnar, P., Royden, L., Yipeng, W., Peizhen, Z., Weiqi, Z., 1989. Intracrustal detachment within zones of continental deformation. Geology 17, 748–751.

Camacho, A., Vernon, R., Fitzgerald, J.D., 1995. Large volumes of anhydrous pseudotachylyte in the Woodroffe thrust, eastern Musgrave Ranges, Australia. Journal of Structural Geology 17, 371–383.

Chamberlain, C.P., Zeitler, P.K., Cooper, A.F., 1995. Geochronologic constraints of the uplift and metamorphism along the Alpine Fault, South Island, New Zealand. New Zealand Journal of Geology and Geophysics 38, 515–523.

Choukroune, P., Gapais, D., 1983. Strain pattern in the Aar Granite (Central Alps) orthogneiss developed by bulk inhomogeneous flattening. Journal of Structural Geology 5, 411–418.

Clark, M.B., Brantley, S.L., Fisher, D.M., 1995. Power-law vein thickness distributions and positive feedback in vein growth. Geology 23, 975–978.

Cooper, A.F., 1974. Multiphase deformation and its relationship to metamorphic crystallization at Haast River, south Westland, New Zealand. New Zealand Journal of Geology and Geophysics 17, 855–880.

Cooper, A.F., 1980. Retrograde alteration of chromium kyanite in metachert and amphibolite whiteschist from the Southern Alps, New Zealand, with implications for uplift on the Alpine Fault. Contributions to Mineralogy and Petrology 75, 153–164.

Cooper, A.F., Barreiro, B.A., Kimbrough, D.L., Mattinson, J.M., 1987. Lamprophyre dike intrusion and the age of the Alpine Fault, New Zealand. Geology 15, 941–944.

Davey, F.J., Henyey, T., Kleffmann, S., Melhuish, A., Okaya, D., Stern, T.A., Woodward, D.J., 1995. Crustal reflections from the Alpine Fault zone, South Island, New Zealand. New Zealand Journal of Geology and Geophysics 38, 601–604.

Davey, F.J., Henyey, T., Holbrook, W.S., Okaya, D., Stern, T.A., Melhuish, A., Henrys, S., Anderson, H., Eberhart-Phillips, D., McEvilly, T., Uhrhammer, R., Wu, F., Jiracek, G.R., Wannamaker, P.E., Caldwell, G., Christensen, N., 1998. Preliminary results from a geophysical study across a modern continent–continent collisional plate boundary—the Southern Alps, New Zealand. Tectonophysics 288, 221–235.

Davis, G.A., Lister, G.S., Reynolds, S.J., 1986. Structural evolution of the Whipple and South Mountains shear zones, southwestern United States. Geology 14, 7–10.

Davison, I., McCarthy, M., Powell, D., Torres, H.H.F., Santos, C.A., 1995. Laminar flow in shear zones: the Pernambuco Shear Zone, NE Brazil. Journal of Structural Geology 17, 149–161.

DeMets, C., Gordon, R.G., Argus, D.F., Stein, S., 1994. Effect of recent revisions to the geomagnetic reversal time scale on estimates of current plate motions. Geophysical Research Letters 21, 2191–2194.

Dewey, J.F., Holdsworth, R.E., Strachan, R.A., 1998. Transpression and transtension zones. In: Holdsworth, R.E., Strachan, R.A., Dewey, J.F.

(Eds.), Continental Transpressional and Transtensional Tectonics. Geological Society of London, Special Publication 135, pp. 1–14.

Ellis, S., Wissing, S., Pfiffner, A., 2001. Strain localisation as a key to reconciling experimentally derived flow-law data with dynamic models of continental collision. International Journal of Earth Sciences 90, 168–180.

Ellis, S.M., Stöckhert, B., 2002. Displacement of the brittle–ductile transition during the earthquake cycle. Eos. Transactions AGU 83(22) Western Pacific Geophysics Meeting Supplement, Abstract SE31B-02.

Flack, C.A., Klemperer, S.L., McGeary, S.E., Snyder, D.B., Warner, M.R., 1990. Reflections from mantle fault zones around the British Isles. Geology 18, 528–532.

Flinn, D., 1965. On the symmetry principle and the deformation ellipsoid. Geological Magazine 102, 36–45.

Fossen, H., Tikoff, B., 1993. The deformation matrix for simultaneous simple shearing, pure shearing and volume change, and its application to transpression–transtension tectonics. Journal of Structural Geology 15, 413–422.

Fossen, H., Tikoff, B., 1998. Extended models of transpression and transtension and applications to tectonic settings. In: Holdsworth, R.E., Strachan, R.A., Dewey, J.F. (Eds.), Continental Transpressional and Transtensional Tectonics. Geological Society of London Special Publication 135, pp. 15–33.

Grapes, R.H., Watanabe, T., 1992. Metamorphism and uplift of Alpine Schist in the Franz Josef–Fox Glacier area of the Southern Alps, New Zealand. Journal of Metamorphic Geology 10, 171–180.

Grapes, R.H., Watanabe, T., 1994. Mineral composition variation in Alpine Schist, Southern Alps, New Zealand: implications for recrystallization and exhumation. The Island Arc 3, 163–181.

Hanmer, S., 1988. Great Slave Lake Shear Zone, Canadian Shield: a reconstructed vertical profile of a crustal scale fault. Tectonophysics 149, 245–264.

Hanmer, S., Bowring, S., van Breeman, O., Parrish, R., 1992. Great Slave Lake shear zone, NW Canada: mylonitic record of Early Proterozoic continental convergence, collision and indentation. Journal of Structural Geology 14, 757–773.

Hanmer, S., Williams, M., Kopf, C., 1995. Modest movements, spectacular fabrics in an intracontinental deep-crustal strike-slip fault: Striding-Athabasca mylonite zone, NW Canadian Shield. Journal of Structural Geology 17, 493–507.

Hauge, T., Allmendinger, R., Caruso, C., Hauser, E., Klemperer, S., Opdyke, S., Potter, C., Sanford, W., Brown, L., Kaufman, S., Oliver, J., 1987. Crustal structure of western Nevada from COCORP deep seismic-reflection data. Geological Society of America Bulletin 98, 320–329.

Hobbs, B., Ord, A., Teyssier, C., 1986. Earthquakes in the ductile regime? Pure and Applied Geophysics 142, 309–336.

Holcombe, R.J., Little, T.A., 2001. A sensitive vorticity gauge using rotated porphyroblasts, and its application to rocks adjacent to the Alpine Fault, New Zealand. Journal of Structural Geology 23, 970–989.

Holm, D.K., Norris, R.J., Craw, D., 1989. Brittle/ductile deformation in a zone of rapid uplift: central Southern Alps, New Zealand. Tectonics 8, 153–168.

Imber, J., Holdsworth, R.E., Butler, C.A., Strachan, R.A., 2001. A reappraisal of the Sibson–Scholz fault zone model: the nature of the frictional to viscous ("brittle–ductile") transition along a long-lived, crustal-scale fault, Outer Hebrides, Scotland. Tectonics 20, 601–624.

Jackson, J.A., 2002. Strength of the continental lithosphere: time to abandon the jelly sandwich? GSA Today 12, 4–10.

Jiang, D., White, J.C., 1995. Kinematics of rock flow and the interpretation of geological structures with particular reference to shear zones. Journal of Structural Geology 17, 1249–1265.

Jiang, D., Lin, S., Williams, P.F., 2001. Deformation path in high-strain zones, with reference to slip partitioning in transpressional plate-boundary regions. Journal of Structural Geology 23, 991–1005.

Jones, D.L., Graymer, R., Wang, C., McEvilley, T.V., Lomax, A., 1994. Neogene transpressive evolution of the Californian Coast Ranges. Tectonics 13, 561–574.

Koons, P.O., 1987. Some thermal and mechanical consequences of rapid uplift: an example from the Southern Alps, New Zealand. Earth and Planetary Science Letters 86, 307–319.

Koons, P.O., 1990. Two-sided orogen: collision and erosion from the sandbox to the Southern Alps, New Zealand. Geology 18, 679–683.

Koons, P.O., Norris, R.J., Craw, D., Cooper, A.F., 2003. Influence of exhumation on the structural evolution of transpressional plate boundaries: an example from the Southern Alps, New Zealand. Geology 31, 3–6.

Lacassin, R., Leloup, P.H., Tapponnier, P., 1993. Bounds on strain in large Tertiary shear zones of SE Asia from boudinage restoration. Journal of Structural Geology 15, 677–692.

Leitner, B.D., Eberhart-Philips, H., Anderson, H., Nabelek, J.N., 2001. A focused look at the Alpine Fault, New Zealand: seismicity, focal mechanisms and stress inversions. Journal of Geophysical Research 106, 2193–2220.

Little, T.A., Holcombe, R.J., Ilg, B.R., 2002. Kinematics of oblique collision and ramping inferred from microstructures and strain in middle crustal rocks, central Southern Alps, New Zealand. Journal of Structural Geology 24, 219–239.

Lynch, J.C., Richards, M.A., 2001. Finite element models of stress orientations in well-developed strike-slip fault zones: implications for the distribution of lower crustal strain. Journal of Geophysical Research 106, 26,707–26,730.

Lynn, H.B., Quam, S., Thompson, G.A., 1983. Depth migration and interpretation of the COCORP Wind River, Wyoming, seismic reflection data. Geology 11, 462–469.

Maggi, A., Jackson, J., McKenzie, D., Priestley, K., 2000. Earthquake focal depths, effective elastic thickness, and the strength of the continental lithosphere. Geology 28, 495–498.

Manning, C.E., 1994. Fractal clustering of metamorphic veins. Geology 22, 335–338.

Mawer, C.K., 1983. State of strain in a quartzite mylonite, Central Australia. Journal of Structural Geology 5, 401–409.

McBride, J.H., Snyder, D.B., England, R.W., Hobbs, R.W., 1996. Dipping reflectors beneath old orogens: a perspective from the British Caledonides. GSA Today 6, 1–6.

McCaffrey, K., Johnston, J.D., Feely, M., 1993. The use of fractal statistics in the analysis of Mo–Cu mineralization at Mace Head, County Galway. Irish Journal of Earth Sciences 12, 139–148.

McGeary, S., 1989. Reflection seismic evidence for a Moho offset beneath the Walls Boundary strike-slip fault. Geological Society of London Journal 146, 261–270.

Molnar, P., Anderson, H.J., Audoine, E., Eberhart-Phillips, D., Gledhill, K.R., Klosko, E.K., McEvilly, T.V., Okaya, D., Savage, M.K., Stern, T., Wu, F.T., 1999. Continuous deformation versus faulting through continental lithosphere: tests using New Zealand as a laboratory for the study of continental dynamics. Science 286, 516–519.

Norris, R.J., Cooper, A.F., 1997. Erosional control on the structural evolution of a transpressional thrust complex on the Alpine Fault, New Zealand. Journal of Structural Geology 19, 1323–1342.

Norris, R.J., Cooper, A.F., 2001. Late Quaternary slip rates and slip partitioning on the Alpine Fault, New Zealand. Journal of Structural Geology 23, 507–520.

Norris, R.J., Koons, P.O., Cooper, A.F., 1990. The obliquely-convergent plate boundary in the South Island of New Zealand: implications for ancient collision zones. Journal of Structural Geology 12, 715–725.

Pfiffner, O.A., Ramsay, J.G., 1982. Constraints on geological strain rates: arguments from finite strain states of deformed rocks. Journal of Geophysical Research 87, 311–321.

Piazolo, S., Passchier, C.W., 2002. Controls on lineation development in low to medium grade shear zones: a study from the Cap de Creus Peninsula, Spain. Journal of Structural Geology 24, 25–44.

Prescott, W.H., Nur, A., 1981. The accommodation of relative motion at

depth on the San Andreas Fault System in California. Journal of Geophysical Research 86, 999–1004.

Prior, D.J., 1988. Deformation processes in the Alpine Fault mylonites, South Island, New Zealand. PhD Thesis, University of Leeds, UK.

Reed, J.J., 1964. Mylonites, cataclasites, and associated rocks along the Alpine Fault, South Island, New Zealand. New Zealand Journal of Geology and Geophysics 7, 645–684.

Sanderson, D.J., Marchini, W.R.D., 1984. Transpression. Journal of Structural Geology 6, 449–458.

Scholz, C., 1988. The brittle–plastic transition and the depth of seismic faulting. Geologische Rundschau 77, 319–328.

Schulz, S.E., Evans, J.P., 2000. Mesoscopic structure of the Punchbowl Fault, Southern California and the geologic and geophysical structure of active strike-slip faults. Journal of Structural Geology 22, 913–930.

Sibson, R.H., 1977. Fault rocks and fault mechanisms. Geological Society of London Journal 133, 191–213.

Sibson, R.H., 1982. Fault zone models, heat flow, and the depth distribution of earthquakes in the continental crust of the United States. Seismological Society of America Bulletin 72, 151–163.

Sibson, R.H., 1983. Continental fault structure and the shallow earthquake source. Geological Society of London Journal 140, 741–767.

Sibson, R.H., White, S.H., Atkinson, B.K., 1979. Fault rock distribution and structure within the Alpine Fault Zone: a preliminary account. In: Walcott, R.I., Cresswell, M.M. (Eds.), The Origin of the Southern Alps. Bulletin of the Royal Society of New Zealand 18, pp. 55–65.

Stern, T., Molnar, P., Okaya, D., Eberhart-Phillips, D., 2000. Teleseismic P-wave delays and modes of shortening the mantle lithosphere beneath South Island, New Zealand. Journal of Geophysical Research 105, 21, 615–21,631.

Sutherland, R., 1994. Displacement since the Pliocene along the southern section of the Alpine fault, New Zealand. Geology 22, 327–331.

Sutherland, R., 1995. The Australia–Pacific boundary and Cenozoic plate motions in the southwest Pacific: some constraints from Geosat data. Tectonics 14, 819–831.

Sutherland, R., Davey, F., Beavan, J., 2000. Plate boundary deformation in South Island, New Zealand, is related to inherited lithospheric structure. Earth and Planetary Science Letters 177, 141–151.

Tippett, J.M., Kamp, P.J.J., 1993. Fission track analysis of the late Cenozoic vertical kinematics of continental Pacific crust, South Island, New Zealand. Journal of Geophysical Research 98, 16,119–16,148.

Unsworth, M.J., Malin, P.E., Egbert, G.D., Booker, J.R., 1997. Internal structure of the San Andreas fault at Parkfield, California. Geology 25, 359–362.

Walcott, R.I., 1978. Present tectonics and late Cenozoic evolution of New Zealand. Geophysical Journal of the Royal Astronomical Society 52, 137–164.

Walcott, R.I., 1998. Modes of oblique compression: late Cenozoic tectonics of the South Island, New Zealand. Reviews of Geophysics 36, 1–26.

Wallace, R.C., 1974. Metamorphism of the Alpine Schist, Mataketake Range, South Westland, New Zealand. Journal of the Royal Society of New Zealand 4, 253–266.

Weijermars, R., 1987. The Palomares brittle–ductile shear zone of southern Spain. Journal of Structural Geology 9, 139–157.

Wellman, H.W., 1947. Sheet mica in South Westland. New Zealand Journal of Science and Technology 28, 236–248.

Wellman, H.W., 1979. An uplift map for the South Island of New Zealand, and a model for uplift of the Southern Alps. In: Walcott, R.I., Cresswell, M.M. (Eds.), The Origin of the Southern Alps. Bulletin of the Royal Society of New Zealand 18, pp. 13–20.

Wenk, H.R., 1998. Deformation of mylonite in Palm Canyon, California, based on xenolith geometry. Journal of Structural Geology 20, 559–571.

White, J.C., 1996. Transient discontinuities revisited: pseudotachylyte, plastic instability and the influence of low pore fluid pressure on deformation processes in the mid-crust. Journal of Structural Geology 18, 1471–1486.

Wittlinger, G., Taponnier, P., Poupinet, G., Mei, J., Damian, S., Herquel, G., Masson, F., 1998. Tomographic evidence for localised lithospheric shear along the Altyn Tagh Fault. Science 282, 74–76.

Woodward, D.J., 1979. The crustal structure of the Southern Alps, New Zealand, as determined by gravity. In: Walcott, R.I., Cresswell, M.M. (Eds.), The Origin of the Southern Alps. Royal Society of New Zealand Bulletin 18, pp. 95–98.

Zandt, G., 1981. Seismic images of the deep structure of the San Andreas Fault System, central Coast Ranges, California. Journal of Geophysical Research 86, 5039–5052.